Predator-induced defence in a dinoflagellate generates benefits without direct costs

Ryderheim, Fredrik; Selander, Erik; Kiørboe, Thomas

Published in:
ISME Journal

Link to article, DOI:
10.1038/s41396-021-00908-y

Publication date:
2021

Document Version
Peer reviewed version

Predator-induced defence in a dinoflagellate generates benefits without direct costs

Fredrik Ryderheim[1*], Erik Selander[2] and Thomas Kiørboe[1]

1) Centre for Ocean Life, DTU Aqua, Technical University of Denmark, Kemitorvet, 2800 Kgs. Lyngby, Denmark

2) University of Gothenburg, Department of Marine Sciences, Carl Skottsbergs gata, 41319 Göteborg, Sweden.

*Correspondence: E-mail: frry@aqua.dtu.dk, telephone: +46725362678

Running head: Defensive benefits without direct costs

Keywords: trade-offs, dinoflagellate, *Alexandrium minutum*, toxin production, copepodamides, defence mechanisms

Conflict of interest

We declare we have no conflict of interest.

This paper has been published:
Ryderheim, F., E. Selander, and T. Kiørboe. 2021. Predator-induced defence in a dinoflagellate generates benefits without direct costs. ISME J 15: 2107–2116. doi:10.1038/s41396-021-00908-y

Abstract

Inducible defences in phytoplankton are often assumed to come at a cost to the organism, but trade-offs have proven hard to establish experimentally. A reason for this may be that some trade-off costs only become evident under resource-limiting conditions. To explore the effect of nutrient limitation on trade-offs in toxin-producing dinoflagellates, we induced toxin production in *Alexandrium minutum* by chemical cues from copepods under different levels of nitrogen limitation. The effects were both nitrogen- and grazer-concentration dependent. Induced cells had higher cellular toxin content and a larger fraction of the cells was rejected by a copepod, demonstrating the clear benefits of toxin production. Induced cells also had a higher carbon and nitrogen content, despite an up to 25% reduction in cell size. Unexpectedly, induced cells seemed to grow faster than controls, likely owing to a higher specific nutrient affinity due to reduced size. We thus found no clear trade-offs, rather the opposite. However, indirect ecological costs that do not manifest under laboratory conditions may be important. Inducing appropriate defence traits in response to threat-specific warning signals may also prevent larger cumulative costs from expressing several defensive traits simultaneously.

Introduction

Dinoflagellates of the genus *Alexandrium* produce neurotoxic alkaloids collectively known as paralytic shellfish toxins (PST). The toxins are efficient sodium-channel blockers and among the most potent toxins known [1]. The intracellular toxin content is up-regulated in response to the level of threat from zooplankton grazers [2] and, while debated, toxicity as a defence mechanism against grazers is the favoured explanation for the evolution of algal toxins [3–6].

Studies dedicated to defence mechanisms in phytoplankton often focus on the benefits of the defence, but rarely establish potential costs [7]. So far, experimental assessments have suggested toxin production trade-offs to be insignificant. The growth rate of toxic and non-toxic strains of the same species, or grazer-induced versus non-induced cells with very different toxin contents appear to be identical [2, 8, 9]. Blossom et al. [10] compared several species and strains of *Alexandrium* spp. and did not find any correlation between growth rate and toxin production under light-replete conditions, and even a positive correlation under limiting light. Brown & Kubanek [11] recently demonstrated a negative relation between toxin content and growth rate in *Alexandrium minutum* exposed to lysed cells of various other species of dinoflagellates, thus suggesting a trade-off. However, the correlation may also result from allelochemical substances in the lysed cells reducing growth [12]. Many dinoflagellates produce such dissolved allelochemicals that reduce the growth rate of other cells [13] and when growth is reduced cells commonly become more toxic [14]. Significant costs of predator-induced toxin production have so far only been convincingly demonstrated in diatoms that produce domoic acid, but here the benefits of the toxins are still debated [15]. However, ecological theory predicts associated costs; otherwise, non-defended species or strains would be outcompeted and only defended species would persist. Also, toxin production is inducible; i.e., it is up-regulated in the presence of grazers cues, as seen in *Alexandrium* spp. dinoflagellates [2, 16, 17] and some toxic strains of the diatom *Pseudo-*

53 *nitzschia* [15, 18]. According to optimal defence theory, inducible defences are favoured
54 when predation risks vary in time and defence costs are significant [19, 20]. While these costs
55 have likely been reduced through evolution, the wide variety of inducible defences found in
56 both marine and terrestrial organisms suggests the presence of influential trade-offs to any
57 beneficial defensive trait [21–24].

58 The failure of experiments to demonstrate costs may be due to the fact that experimental
59 assessments have often been done under resource-replete conditions, while costs may be
60 more significant when resources are limited [7, 20, 25–27]. The PST molecules are high in
61 nitrogen with N:C ratio 4.6 times higher than average phytoplankton materials [28].
62 Numerous studies have shown cell toxin content to be low in nitrogen-depleted cells [29, 30]
63 even when exposed to a grazer threat [9]. Trade-off costs may be trivial when nutrients and
64 light are plentiful, but when available nitrogen is limiting and grazer biomass high, a fitness-
65 optimization resource-allocation model predicts a significant growth penalty to toxin
66 production [31]. Nitrogen limitation in temperate shelf regions generally occurs during the
67 summer months [32, 33], and coincidentally it is during these months that defence is most
68 needed due to peaking copepod biomass [33, 34].

69 Here, we quantify the benefits and costs of toxin production in *Alexandrium minutum* under
70 different degrees of nitrogen limitation using both a chemostat approach and classical batch
71 experiments. The compounds from zooplankton that trigger toxin production are known [35],
72 and we use them for precise manipulation of toxin production without confounding effects of
73 grazing on fitness estimates. The efficiency of the defence is estimated by video recording the
74 response of copepods to induced and non-induced cells. Following the predictions of the
75 model of Chakraborty et al. [31], we hypothesize that the costs of increased toxicity of
76 induced cells will be highest at intermediate nitrogen limitation, and that cells grown in
77 excess of nitrogen will reap full benefit while paying negligible costs.

Materials and methods

Phytoplankton

Alexandrium minutum strain GUMACC 83 were grown in B1 medium [36] at salinity 26, 18 °C, and an irradiance of *ca*. 150 µmol photons m^{-2} s^{-1} on a 12:12 light:dark cycle. To reduce carry-over of nitrogen from the stock culture we diluted cells in B1 with reduced NO_3^- (80 µM) for two weeks prior to inoculation and used cells that were close to the end of the exponential phase.

Batch-culture experiment

Six replicate batch cultures of *A. minutum* were initiated at *ca*. 200 cells mL^{-1} in 2 L blue-cap glass flasks exposed to *ca*. 150 µmol photons m^{-2} s^{-1} on a 12:12 light:dark cycle and constant temperature of 18 °C. We used modified B1 medium with reduced nitrogen concentration (60 µM NO_3^-) to make sure that the cells eventually would be limited by nitrogen rather than other resources. The cultures were gently bubbled to avoid high pH limiting growth. pH was monitored using a PHM220 Lab pH meter (Radiometer Analytical, Lyon, France). Three bottles were treated with copepodamides to induce increased toxin production [35] and three were used as controls. Copepodamides were extracted from freeze-dried *Calanus finmarchius* (Calanus AS, Tromsø, Norway) as described in Selander et al. [35] and added to the cultures by coating the inside of the bottle with a copepodamide mixture dissolved in methanol to a final concentration of 2 nM. Due to slow release and rapid degradation the average effective concentration is around 1−2% of the added concentration [18]. The methanol was evaporated using N_2 gas and the cultures transferred to the bottles after gentle mixing. Cultures were gently transferred to a freshly coated flasks every 24 hours during the treatment period to assure a continuous exposure to the cues [18]. The controls received the same treatment but with methanol without copepodamides. Samples were taken every or every second day for

cell abundance and nitrogen concentration while samples for toxin analysis and cellular carbon and nitrogen were taken at inoculation and in conjunction with the six video experiments (see below) during the course of the experiment. Initial samples of cellular toxin-, carbon-, and nitrogen content were taken from the stock culture.

Chemostat experiments

While nutrient concentration declines over time in batch cultures, they are near constant in a continuous culture, thus allowing us to examine costs and benefits of grazer induction at constant concentrations of nutrients. Dinoflagellates do not tolerate vigorous mixing [37], so a classical chemostat cannot be used. Instead, we used exponentially fed batch cultures [38]. The exponentially fed batch culture (hereafter referred to as 'chemostat') is similar to a chemostat except that there is no continuous outflow. The volume is instead reduced to the initial volume at each sampling occasion after gently mixing the culture. Growth medium is added continuously in a constant proportion of the increasing volume of the culture by exponentially increasing the inflow using a computer controllable multichannel peristaltic pump (IPC 16, Ismatec, Wertheim, Germany).

Six replicate chemostat cultures of *A. minutum* were set up as in 1-L blue-cap glass bottles as described above. Depending on the dilution rate (DR), the initial culture volume varied between 250−500 mL. Four different DR were used to vary cell growth rate: 0.05, 0.10, 0.20, and 0.40 d^{-1}. The inflow medium was B1 with reduced (80 µM) NO_3^- in all the experiments except the first one (0.10 d^{-1} DR) where the NO_3^- concentration was 30 µM. We increased the nitrogen concentration in the subsequent experiments as this allowed more cells for analyses and because pH limitation turned out not to be a problem. The resulting ambient nitrogen concentration is independent on nitrogen content of the inflow medium (Appendix 1). The cultures were gently bubbled and pH was measured at each sampling occasion. At

each DR, the cultures were allowed seven to ten days to achieve steady-state before starting the experimental treatment. In some cases perfect steady-state was not achieved.

The cultures were exposed to copepodamides daily as described above, using a nominal concentration of 0.63 nM. For the 0.2 d^{-1} DR a second experiment was run with higher copepodamide concentration of 6 nM to analyse the effect of increased exposure to grazers. Samples for analysis of cell abundance and size, cell toxin content, cellular carbon and nitrogen, dissolved inorganic nitrogen, and copepod rejection rate were taken daily or every 2–3 days during the 6–10 day treatment period. Using the chemostat equations (Appendix 1) and assuming a maximum growth rate of 0.5 d^{-1} [39] and a half-saturation constant for nitrate of 0.5 μM [40] the resulting nitrate concentration in the cultures should range from severe limitation to saturation. Thus, while nutrient concentration decrease over time in batch culture, it is more constant and controlled by the dilution rate in chemostats.

In the chemostats, the growth rate is controlled by the DR and any growth rate response will manifest as a change in the steady-state concentrations of cells and nutrients. Thus, if induced toxin production cause lower growth or nutrient affinity, the steady-state concentration of nutrients will increase and cell density decrease. The magnitude of the response can be computed from the chemostat equations (Appendix 1).

Cell counts and cell size

Cell concentrations were determined in acid Lugol (1%) fixed samples. All cells in one mL or at least 400 cells were counted per replicate in a Sedgewick-Rafter chamber using an inverted microscope (Olympus, Tokyo, Japan). 20 random cells from each sample were measured at 400× magnification (width-length) and cell volume was estimated by assuming a prolate-spheroid shape [41]. Cell growth was calculated from temporal differences in cell

concentration assuming exponential growth. The dilution rate was accounted for when calculating growth in the chemostat experiments.

Nitrate analysis

Subsamples for nitrate analysis were filtered through a 0.2-µm syringe filter, and stored frozen at –20 °C until analysis. Nitrate was analysed by reduction to NO_x with VCl_3 as the reducing reagent [42] on a Smartchem 200 (AMS Alliance, Rome, Italy). Concentrations below 0.5 µM were measured using an extended cuvette (100 mm, FireflySci, New York, New York, USA) by UV-VIS spectrophotometry.

Toxin analysis

Samples (10−120 mL) for cellular toxin contents were filtered onto 25 mm Whatman GF/F glass fibre filters and frozen at –20 °C until extraction. 750 µL of 0.05 M acetic acid was added and samples were subjected to three freeze-thaw cycles to lyse cells. The extracts were filtered (GF/F) and stored at –20 °C until analysis. The samples from the batch experiment and the 0.2 d^{-1} DR experiments (both low and high dose) were analysed with isocratic ion-pair chromatography followed by post-column derivatization and fluorescent detection [43]. We used a reversed phase C18 column (150×4 mm C18, 5 µm, Dr. Maisch GmBH, Ammerbuch, Germany). Samples from the 0.05, 0.10, and 0.40 d^{-1} DR experiments were separated on an Agilent 1200 HPLC (ZIC-HILIC, 2.1×150 mm, 5 µm, Merck KGaA, Darmstadt, Germany) and analysed by tandem mass spectrometry on a triple-quadrupole instrument (Agilent 6470) following the methods described in [44].

This particular strain of *A. minutum* is known to only produce gonyautoxins (GTX) 1–4 [2, 45]. GTX standards 1–4 were obtained from the Certified Reference Materials Program at National Research Council Canada (Halifax, Canada).

Cellular carbon and nitrogen

Samples for cellular C and N were filtered onto pre-combusted (550 °C, 2 hours) 13 mm GF/C filters, packed in tin capsules and dried for 24 hours at 60 °C. The samples were kept dry at room temperature in a desiccator until analysis with a Thermo Scientific Flash 2000 Organic Elemental Analyzer (Thermo Fisher Scientific, Waltham, Massachusetts, USA).

Copepod feeding response

We directly observed individual copepod-cell interactions and recorded the fraction of captured cells that were rejected. We used the feeding-current feeding copepod *Temora longicornis* from a continuous culture that was maintained on a phytoplankton diet consisting of *Rhodamonas salina*, *Thalassioria weissflogii*, *Heterocapsa triquetra*, and *Oxyrrhis marina.*

Adult female copepods were tethered to a human hair by their dorsal surface using cyanoacrylate-based super glue [46]. The tethered copepods were starved overnight in darkness at the same temperature (18 °C) and salinity (26) as the cultures before being used for experiments. The tethered copepods are seemingly unaffected by the tethering and can live for many days while feeding, defecating, and producing eggs.

The feeding experiments took place in darkness. The untethered end of the hair was glued to a needle attached to a micromanipulator. The copepod was submerged in a 10×10×10 cm^3 aquarium and *Alexandrium* cells were added to a final concentration of 100-200 cells mL^{-1}. The experiment started when cells were added. The water was gently mixed by a magnetic stirrer to keep the cells suspended. Three 10-minute sequences (0-10 minutes, 25-35 minutes, and 50-60 minutes) of 24 fps footage was recorded during a one-hour period using a high-speed camera (Phantom V210; Vision Research, Wayne, New Jersey, USA) connected to a computer. The camera was equipped with lenses to get a field of view of 1.3 × 1 mm^2. The

196 video sequences were analysed to quantify prey capture, ingestion, and the fraction of cells
197 that were rejected by the copepod [46]. A new copepod was used for each replicate culture.

198 *Statistical analysis*

199 The effect of the copepodamide treatment in the batch-culture experiment was analysed using
200 a generalized additive mixed model (GAMM) in the '*gamm4*' R package [47]. 'Treatment'
201 and 'Time' were used as fixed effects and 'Replicate' as the random effect.

202 To analyse the effect of the copepodamide treatment in the chemostat experiments, we used a
203 linear mixed effects model with 'Time', 'Treatment', and 'Dilution rate' as fixed effects, and
204 'Replicate' as the random effect, in the '*lmerTest'* R package [48]. The analysis of the
205 repeated 'High' copepodamide-dose experiment was done separately. The Akaike
206 information criterion was used to select the model that best fit the data. In case of a
207 significant interaction between 'Dilution rate' and 'Treatment' a post-hoc test was made via
208 pairwise comparisons by estimated marginal means using the Satterthwaite degrees of
209 freedom method. The random-effect-variance component was close to zero for some
210 variables, but retained in the model to incorporate the dependency of the response variable on
211 the replications. Some variables were log-transformed to homogenize variances. Statistical
212 tests were considered significant at the 0.05 level and are summarized in Appendix Tables
213 S1, S2, S3 and S4.

214 **Results**

215 *Batch-culture experiment*

216 Cell abundance in the grazer-induced cultures increased faster than controls during the
217 exponential phase (days 3–12; GAMM, $F = 14.0$, $p < 0.001$) and reached the stationary phase
218 after around 14 days as the inorganic nitrogen in the cultures became depleted (Fig. 1a, c).
219 The available nitrate in the culture medium was used up at a significantly higher rate in the

induced treatment (Fig. 1c; GAMM, $F = 9.7$, $p = 0.003$), because cell accumulation rate in terms of cellular nitrogen was also faster in induced than in non-induced cultures (Appendix 2 Fig. S1; GAMM, $F = 11.0$, $p = 0.003$). Cellular nitrogen content and cell sizes initially increased and then decreased as nutrients were exhausted and growth ceased, but induced cells had a significantly higher nitrogen content (Fig. 1d) and were significantly smaller (Fig. 1g, Appendix 2 Table S1) than non-induced cells during the exponential growth phase but converged with control cells after 10 and 16 days, respectively. Cellular carbon content was significantly higher in induced than in non-induced cells (Fig. 1e, Appendix 2 Table S1), resulting also in a faster accumulation of biomass during the exponential phase (Appendix 2 Fig. S1; GAMM, $F = 61.8$, $p < 0.001$). The differences in cellular C and N contents between induced and non-induced cultures on a per-cell level showed the same pattern, but were less pronounced (Appendix 2 Fig. S1). The carbon to nitrogen ratio also increased in response to nitrate depletion but more markedly so in induced treatments (Fig. 1f). Overall, cellular nitrogen content increased and cellular carbon content decreased with increasing growth rate and the contents of both nitrogen and carbon were higher in induced cells (Fig. 2, Appendix Table S2).

Cell toxicity peaked after six days of exposure in the induced treatments with 400% higher GTX content than controls, after which it decreased throughout the rest of the exponential phase (Fig. 1h). Toxin production essentially reached zero after 14 days but cell toxicity remained stable at around 5–7 amol μm^{-3} due to the low cell division rates. In the control treatment, cell toxicity followed the same temporal patterns but was lower throughout than in induced cells (Fig. 1h). Finally, a significantly higher fraction of induced than non-induced cells were rejected by copepods, demonstrating a clear benefit (Fig. 1i).

Chemostat experiments

Growth rate in the 0.05, 0.10, and 0.40 d^{-1} DR experiments were lower than the DR and cell concentrations thus decreased over time (Fig. 3). It was only in the two 0.20 d^{-1} DR experiments that the cells were able to keep up with the DR (Fig. 3c, Fig. 4a). However, growth rates calculated from cell-bound nitrogen values per culture volume (µg N mL^{-1}) were nearly constant over time at the three lowest DR, and the growth rates were similar to the DR except at the lowest and highest DR (Figure 4b, Appendix 2 Fig. S2). The small differences in cell concentrations and the low sensitivity of estimates of affinity and maximum growth rate parameters to changes in cell concentration at low DR makes the estimation of these parameters meaningless (Appendix 1).

Consistent with the results of the batch-experiment results, induced cells were significantly smaller than non-induced cells at intermediate DR but similar at the lowest and highest rates. (Figure 4c). Cellular carbon increased and nitrogen contents decreased with growth rate and both were significantly higher in induced than non-induced cells, particularly at intermediate DR (Figure 4d, e, Fig. 2). Cellular C:N ratio varied inversely with DR and were slightly higher in induced than non-induced cells, all again consistent with the patterns in the batch experiment (Figure 4f, Fig. 2). As in the batch experiment, effects were similar but less pronounced when expressed on a per-cell basis (Appendix 2 Table S5, S6). The effect of varying the copepodamide dose from low (0.63 nM) to high (6 nM) in the 0.2 d^{-1} DR experiment had a significant effect on (reduced) cell volume and also further increased toxin content relative to the controls (Fig. 4c, g; Appendix 2 Table S4), consistent with the result of a more comprehensive dose-response experiment (Appendix 3; Appendix 3. Fig. S1).

Cell toxin content increased in all but the 0.05 and 0.10 d^{-1} DR experiments in response to copepodamides (Fig. 4g). Consequently, the copepods generally rejected a larger fraction of induced cells, except at the lowest DR (Fig. 4h; Appendix 2 Table S3, S4). Overall, the

fraction of rejected cells increased with increasing toxin content but the effect saturates at a rather low toxin content of ca. 10 amol GTX μm^{-3} (Fig. 5).

Discussion

We set out to quantify the costs and benefits of toxin production in a dinoflagellate by comparing the performance of cells induced to express their defence with those that were not under different degrees of nitrogen limitation. Our experiments produced decreasing growth rates with increasing nitrogen limitation in both batch and chemostat cultures (Fig. 2a, c), and high C:N ratios in N-limited cells (Fig. 1f, Fig. 4f). We have utilized that toxin-production in many dinoflagellates, including *A. minutum*, can be induced by grazer cues [2, 35], thus allowing us to examine the same strain at different toxin-production rates. This is important because different strains of the same species may differ in many traits, including in their toxin profiles [45, 49]. We note also that we examine the 'private-good' [50] grazer-deterrent effect of the defence at the level of the individual. That is, we quantify the benefits that only the individual cell that produces the toxin may benefit from. This is different from any toxic effects on the copepod that reduce its ability to graze on further cells, which is a 'public good', as also cells not producing the toxin may benefit [50]. We had predicted that both benefits and costs would be small in nutrient-starved cells, that benefits would be large but costs relatively small in nutrient-replete cells, and that both benefits and costs would be high at intermediate nitrogen levels. In line with our hypothesis, toxin-induction was highest at intermediate nitrogen limitation, but we found no evidence of direct costs in terms of reduced growth rate.

Defence trade-offs

The benefits of toxin production were clear and largely followed the pattern predicted. Moreover, the results were consistent between the two types of experiments: induced cells

have up to 3 times higher chance of being rejected by the copepod than non-induced cells, and the chance of rejection was positively correlated to the toxin content of the cells. This confirms previous reports of reduced grazing on induced dinoflagellates [2], but the demonstration at the individual cell level is novel. It is well established that nitrogen-starved cells produce no or very little toxins [9, 51] and, hence, gain little or no defensive benefits. In the batch experiment, cells remained toxic even in the stationary phase due to low cell division rate, but they did not produce new toxins. With low toxin content but high rejection fraction, the 0.1 d^{-1} DR experiment shows some odd behaviour. Thus, we cannot exclude the possibility that other defences, such as allelochemicals [52, 53], are also at play.

The efficiency of the defence was not as high as that reported for other strains and species of *Alexandrium* spp. Thus, Xu and Kiørboe [5] found that more than 90% of the cells of some toxic *Alexandrium* species/strains were rejected by a copepod, but also that other strains containing toxins were readily consumed by the copepod. Neither Xu et al. [46] nor Teegarden et al. [54] were consequently able to relate the efficiency of the defence to the composition and concentration of specific toxins in the cells of *Alexandrium* spp. Here, we have established a direct correlation between the cells' content of the GTX toxin and the efficiency of the defence in the same strain of *Alexandrium minutum*.

It has been notoriously difficult to demonstrate the cost part of defence trade-offs in phytoplankton [7], and this study is no exception, despite a novel approach. Ideally, 'costs' should be quantified in terms of reduced cell division rate. We found no reduction in the growth rate nor in nutrient affinity of the cells, even at nutrient-deplete conditions. The proportion of cellular nitrogen invested in toxins increased the more toxic the cells were (Appendix 2 Fig. S3), but this did not affect growth rate.

However, we document a number of very clear effects of induction in addition to enhanced toxin production, i.e., elevated cellular contents of C and N, a reduction in cell size, and even an increase in cell division rate, with the effects being most pronounced at intermediate nutrient levels. The responses are consistent between the batch and the continuous cultures.

The expectation of reduced cell division rate of grazer-induced, nitrogen-limited cells is based on the nitrogen requirements for PST production in *Alexandrium tamarense* as worked out by Chakraborty et al. [31]. However, *A. tamarense* produce 1-2 orders-of-magnitude more toxins than the *A. minutum* used here. Thus, the biochemical syntheses costs and the N requirements for toxins are correspondingly smaller in our experiment and the higher N-uptake of induced cells cannot be explained by direct requirements for toxin production.

It is well established that cell size decrease when nutrient are limited [55, 56], as also seen most clearly in the batch experiment (Fig. 1g). However, cell volume shrink in response to grazer cues by up to 25% relative to non-induced cells. This has two implications. First, a smaller cell volume results in a higher concentration of toxins in the cells. It is reasonable to assume that the copepods respond to the concentration rather than the contents of toxins, and the shrinking of the cells may therefore be adaptive and part of the defence. A similar consistent response in cell size to grazer cues has been found in four species of diatoms [24]. For the diatoms, smaller cell sizes implies higher concentrations of biogenic silica and, therefore, a stronger protective shell that makes the cells less susceptible to copepod grazing [23].

The second potential implication of cell shrinking is a higher specific affinity for dissolved nutrients. To first order, specific affinity scales inversely with cell radius due to the nature of molecular diffusion [57] and it is well established experimentally that the volume-specific nutrient uptake indeed increases with decreasing cell size [58, 59]. Thus, a 25% decrease in

cell volume, corresponds to an 8% decrease in radius and a corresponding increase in specific affinity. This, in fact, may account for the elevated nitrogen uptake, nitrogen content, and growth rate of induced cells when cells start being nutrient limited, as most clearly seen in the batch experiment (Fig. 1). If the decrease in cell size is an adaptation to increased toxin concentration, then the elevated nitrogen assimilation and growth rate of induced cells is a secondary and beneficiary effect.

The increased carbon content found in induced cells may be due to thickening of their thecal plates, providing them with another possible defence. It is unclear if this has an effect on the copepods, but it has been shown that diatoms that increase their silica shell thickness experience reduced grazing from both juvenile and adult copepods [23].

Ecological and indirect costs of defence

While we were unable to demonstrate direct costs of toxin production even in nitrogen-starved cells, defences may come with indirect ecological costs that do not manifest in simplified laboratory settings [21]. This includes, e.g., increased sinking rate or reduced swimming speed that may inflict fitness costs in nature [60, 61]. A possible ecological cost of the reduced cell size recorded here is elevated predation risk. In general, mortality rate of plankton organisms scale inversely with their volume to power 0.25 [62], and a 25% decrease in volume thus implies a 7.5% increase in predation mortality from other predators than copepods. Copepods and other larger herbivores are probably the most important grazers on dinoflagellates, thus the more than 50% decrease in copepod grazing pressure of induced cells more than outweighs the cost in most situations, and toxin production increases the fitness of the cell.

Theory of defences predicts that defences should only be inducible if they are associated with a cost [63]. The number of studies unable to detect costs associated with induced toxin

production in phytoplankton suggests that additional factors may be at play. Recent advancements in genome sequencing reveals that a substantial part of the genome may be dedicated to secondary metabolism, up to one fifth in some cyanobacteria [64]. Keeping a single biosynthetic pathway active may inflict a very limited cost whereas the cost for constant activation of one fifth of the genome will be substantial [65]. Thus, the evolution of inducible defence may be driven not by the allocation of resources to a single pathway, but the necessity to avoid allocation to all defence systems simultaneously. This is but a corollary hypothesis to the optimal defence theory, but one that may explain the lack of detectable costs in some induced responses to herbivory.

In conclusion, we found a diverse nutrient-dependent response of a dinoflagellate to copepod cues: increased toxicity with implied lower predation risk, higher cellular contents of carbon and nitrogen, reduced cell size, and higher growth rate. Most of these responses may be beneficial to the cells, while we found no indication of direct costs. Because dinoflagellates are not Darwinian demons, the necessary costs are most likely indirect or ecological that are apparent only in nature.

Acknowledgements

The Centre for Ocean Life is supported by the Villum Foundation. ES was funded by Swedish Research Council VR no. 2019-05238. We thank Benni Winding Hansen for CHN measurements, Jack Melbye for maintaining copepod cultures, Colin Stedmon for assistance with NO_3^- measurements, Josephine Grønning for copepodamide extractions, Aurore Maureaud for providing the script for the mixed model, Daniël van Denderen for providing statistical assistance, and Per Juel Hansen for rewarding discussions.

Conflict of interest

We declare we have no conflict of interest.

References:

1. Llewellyn LE. Saxitoxin, a toxic marine natural product that targets a multitude of receptors. *Nat Prod Rep* 2006; **23**: 200–218.
2. Selander E, Thor P, Toth G, Pavia H. Copepods induce paralytic shellfish toxin production in marine dinoflagellates. *Proc R Soc B* 2006; **273**: 1673–1680.
3. Turner JT, Tester PA. Toxic marine phytoplankton, zooplankton grazers, and pelagic food webs. *Limnol Oceanogr* 1997; **42**: 1203–1213.
4. Smetacek V. A Watery Arms Race. *Nature* 2001; **441**: 745.
5. Xu J, Kiørboe T. Toxic dinoflagellates produce true grazer deterrents. *Ecology* 2018; **99**: 2240–2249.
6. Cusick KD, Widder EA. Bioluminescence and toxicity as driving factors in harmful algal blooms: Ecological functions and genetic variability. *Harmful Algae* 2020; **98**: 101850.
7. Pančić M, Kiørboe T. Phytoplankton defence mechanisms: traits and trade-offs: Defensive traits and trade-offs. *Biol Rev* 2018; **93**: 1269–1303.
8. John EH, Flynn KJ. Growth dynamics and toxicity of *Alexandrium fundyense* (Dinophyceae): the effect of changing N:P supply ratios on internal toxin and nutrient levels. *Eur J Phycol* 2000; **35**: 11–23.
9. Selander E, Cervin G, Pavia H. Effects of nitrate and phosphate on grazer-induced toxin production in *Alexandrium minutum*. *Limnol Oceanogr* 2008; **53**: 523–530.
10. Blossom HE, Markussen B, Daugbjerg N, Krock B, Norlin A, Hansen PJ. The Cost of Toxicity in Microalgae: Direct Evidence From the Dinoflagellate *Alexandrium*. *Front Microbiol* 2019; **10**: 1065.
11. Brown ER, Kubanek J. Harmful alga trades off growth and toxicity in response to cues from dead phytoplankton. *Limnol Oceanogr* 2020; lno.11414.
12. Windust AJ, Wright JLC, McLachlan JL. The effects of the diarrhetic shellfish poisoning toxins, okadaic acid and dinophysistoxin-1, on the growth of microalgae. *Mar Biol* 1996; **126**: 19–25.

13. Legrand C, Rengefors K, Fistarol GO, Granéli E. Allelopathy in phytoplankton - biochemical, ecological and evolutionary aspects. *Phycologia* 2003; **42**: 406–419.
14. John E, Flynn K. Modelling changes in paralytic shellfish toxin content of dinoflagellates in response to nitrogen and phosphorus supply. *Mar Ecol Prog Ser* 2002; **225**: 147–160.
15. Lundholm N, Krock B, John U, Skov J, Cheng J, Pančić M, et al. Induction of domoic acid production in diatoms—Types of grazers and diatoms are important. *Harmful Algae* 2018; **79**: 64–73.
16. Bergkvist J, Selander E, Pavia H. Induction of toxin production in dinoflagellates: the grazer makes a difference. *Oecologia* 2008; **156**: 147–154.
17. Griffin JE, Park G, Dam HG. Relative importance of nitrogen sources, algal alarm cues and grazer exposure to toxin production of the marine dinoflagellate *Alexandrium catenella*. *Harmful Algae* 2019; **84**: 181–187.
18. Selander E, Berglund EC, Engström P, Berggren F, Eklund J, Harðardóttir S, et al. Copepods drive large-scale trait-mediated effects in marine plankton. *Sci Adv* 2019; **5**: eaat5096.
19. Rhoades DF. Evolution of plant chemical defense against herbivores. *Herbivores: Their Interaction with Secondary Plant Metabolites*. 1979. Academic Press, New York, NY, pp 1–55.
20. Karban R. The ecology and evolution of induced resistance against herbivores: Induced resistance against herbivores. *Funct Ecol* 2011; **25**: 339–347.
21. Strauss SY, Rudgers JA, Lau JA, Irwin RE. Direct and ecological costs of resistance to herbivory. *TREE* 2002; **17**: 278–285.
22. Agrawal AA. Current trends in the evolutionary ecology of plant defence. *Funct Ecol* 2011; **25**: 420–432.
23. Pančić M, Torres RR, Almeda R, Kiørboe T. Silicified cell walls as a defensive trait in diatoms. *Proc R Soc B* 2019; **286**: 20190184.
24. Grønning J, Kiørboe T. Diatom defence: Grazer induction and cost of shell-thickening. *Funct Ecol* 2020; 1365-2435.13635.
25. Kiørboe T, Andersen KH. Nutrient affinity, half-saturation constants and the cost of toxin production in dinoflagellates. *Ecol Lett* 2019; **22**: 558–560.

441 26. Wang X, Wang Y, Ou L, He X, Chen D. Allocation Costs Associated with Induced Defense in
442 *Phaeocystis globosa* (Prymnesiophyceae): the Effects of Nutrient Availability. *Sci Rep* 2015; **5**:
443 10850.
444 27. Zhu X, Wang J, Chen Q, Chen G, Huang Y, Yang Z. Costs and trade-offs of grazer-induced
445 defenses in *Scenedesmus* under deficient resource. *Sci Rep* 2016; **6**: 22594.
446 28. Redfield AC. The biological control of chemical factors in the environment. *Am Sci* 1958; **46**:
447 205–221.
448 29. Boyer GL, Sullivan JJ, Andersen RJ, Harrison PJ, Taylor FJR. Effects of nutrient limitation on
449 toxin production and composition in the marine dinoflagellate *Protogonyaulax tamarensis*. *Mar*
450 *Biol* 1987; **96**: 123–128.
451 30. Leong SCY, Murata A, Nagashima Y, Taguchi S. Variability in toxicity of the dinoflagellate
452 *Alexandrium tamarense* in response to different nitrogen sources and concentrations. *Toxicon*
453 2004; **43**: 407–415.
454 31. Chakraborty S, Pančić M, Andersen KH, Kiørboe T. The cost of toxin production in
455 phytoplankton: the case of PST producing dinoflagellates. *ISME J* 2019; **13**: 64–75.
456 32. Andersson L. Trends in nutrient and oxygen concentrations in the Skagerrak-Kattegat. *Journal*
457 *of Sea Research* 1996; **35**: 63–71.
458 33. Tiselius P, Belgrano A, Andersson L, Lindahl O. Primary productivity in a coastal ecosystem: a
459 trophic perspective on a long-term time series. *J Plankton Res* 2016; **38**: 1092–1102.
460 34. Kiørboe T, Nielsen TG. Regulation of zooplankton biomass and production in a temperate,
461 coastal ecosystem. 1. Copepods. *Limnol Oceanogr* 1994; **39**: 493–507.
462 35. Selander E, Kubanek J, Hamberg M, Andersson MX, Cervin G, Pavia H. Predator lipids induce
463 paralytic shellfish toxins in bloom-forming algae. *Proc Natl Acad Sci USA* 2015; **112**: 6395–
464 6400.
465 36. Hansen PJ. The red tide dinoflagellate *Alexandrium tamarense*: effects on behaviour and growth
466 of a tintinnid ciliate. *Mar Ecol Prog Ser* 1989; **53**: 105–116.

37. Berdalet E, Peters F, Koumandou VL, Roldán C, Guadayol Ò, Estrada M. Species-specific physiological response of dinoflagellates to quantified small-scale turbulence [1]. *J Phycol* 2007; **43**: 965–977.
38. Fischer R, Andersen T, Hillebrand H, Ptacnik R. The exponentially fed batch culture as a reliable alternative to conventional chemostats. *Limnol Oceanogr Meth* 2014; **12**: 432–440.
39. Flynn K, Jones KJ, Flynn KJ. Comparisons among species of *Alexandrium* (Dinophyceae) grown in nitrogen- or phosphorus-limiting batch culture. *Mar Biol* 1996; **126**: 9–18.
40. Brandenburg KM, Wohlrab S, John U, Kremp A, Jerney J, Krock B, et al. Intraspecific trait variation and trade-offs within and across populations of a toxic dinoflagellate. *Ecol Lett* 2018; **21**: 1561–1571.
41. Hillebrand H, Dürselen C-D, Kirschtel D, Pollingher U, Zohary T. Biovolume Calculation for Pelagic and Benthic Microalgae. *J Phycol* 1999; **35**: 403–424.
42. Schnetger B, Lehners C. Determination of nitrate plus nitrite in small volume marine water samples using vanadium(III)chloride as a reduction agent. *Mar Chem* 2014; **160**: 91–98.
43. Asp TN, Larsen S, Aune T. Analysis of PSP toxins in Norwegian mussels by a post-column derivatization HPLC method. *Toxicon* 2004; **43**: 319–327.
44. Turner A, Tölgyesi L. Determination of Paralytic Shellfish Toxins and Tetrodotoxin in Shellfish using HILIC/MS/MS (Application Note No. 5994-0967EN). 2019.
45. Franco JM, Fernández P, Reguera B. Toxin profiles of natural populations and cultures of *Alexandrium minutum* Halim from Galician (Spain) coastal waters. *J Appl Phycol* 1994; **6**: 275–279.
46. Xu J, Hansen PJ, Nielsen LT, Krock B, Tillmann U, Kiørboe T. Distinctly different behavioral responses of a copepod, *Temora longicornis*, to different strains of toxic dinoflagellates, *Alexandrium* spp. *Harmful Algae* 2017; **62**: 1–9.
47. Wood S, Scheipl F. gamm4: Generalized additive mixed models using mgcv and lme4. 2020.
48. Kuznetsova A, Brockhoff PB, Christensen RHB. **lmerTest** Package: Tests in Linear Mixed Effects Models. *J Stat Soft* 2017; **82**.

494 49. Wohlrab S, Selander E, John U. Predator cues reduce intraspecific trait variability in a marine
495 dinoflagellate. *BMC Ecol* 2017; **17**: 8.
496 50. Driscoll WW, Hackett JD, Ferrière R. Eco-evolutionary feedbacks between private and public
497 goods: evidence from toxic algal blooms. *Ecol Lett* 2016; **19**: 81–97.
498 51. Flynn K, Franco J, Fernandez P, Reguera B, Zapata M, Wood G, et al. Changes in toxin content,
499 biomass and pigments of the dinoflagellate *Alexandrium minutum* during nitrogen refeeding and
500 growth into nitrogen or phosphorus stress. *Mar Ecol Prog Ser* 1994; **111**: 99–109.
501 52. Tillmann U, John U. Toxic effects of *Alexandrium* spp. on heterotrophic dinoflagellates: an
502 allelochemical defence mechanism independent of PSP-toxin content. *Mar Ecol Prog Ser* 2002;
503 **230**: 47–58.
504 53. Tillmann U, Hansen PJ. Allelopathic effects of *Alexandrium tamarense* on other algae: evidence
505 from mixed growth experiments. *Aquat Microb Ecol* 2009; **57**: 101–112.
506 54. Teegarden GJ, Campbell RG, Anson DT, Ouellett A, Westman BA, Durbin EG. Copepod
507 feeding response to varying *Alexandrium* spp. cellular toxicity and cell concentration among
508 natural plankton samples. *Harmful Algae* 2008; **7**: 33–44.
509 55. Peter KH, Sommer U. Interactive effect of warming, nitrogen and phosphorus limitation on
510 phytoplankton cell size. *Ecol Evol* 2015; **5**: 1011–1024.
511 56. Garcia NS, Bonachela JA, Martiny AC. Interactions between growth-dependent changes in cell
512 size, nutrient supply and cellular elemental stoichiometry of marine *Synechococcus*. *ISME J*
513 2016; **10**: 2715–2724.
514 57. Kiørboe T. Turbulence, Phytoplankton Cell Size, and the Structure of Pelagic Food Webs. *Adv*
515 *Mar Biol* 1993; **29**: 1–72.
516 58. Lindemann C, Fiksen Ø, Andersen KH, Aksnes DL. Scaling Laws in Phytoplankton Nutrient
517 Uptake Affinity. *Front Microbiol* 2016; **3**: 1–6.
518 59. Edwards KF, Thomas MK, Klausmeier CA, Litchman E. Allometric scaling and taxonomic
519 variation in nutrient utilization traits and maximum growth rate of phytoplankton. *Limnol*
520 *Oceanogr* 2012; **57**: 554–566.

60. Lürling M, Van Donk E. Grazer-induced colony formation in *Scenedesmus*: are there costs to being colonial? *Oikos* 2000; **88**: 111–118.
61. Selander E, Jakobsen HH, Lombard F, Kiorboe T. Grazer cues induce stealth behavior in marine dinoflagellates. *Proc Natl Acad Sci USA* 2011; **108**: 4030–4034.
62. Kiørboe T. A Mechanistic Approach to Plankton Ecology. 2008. Princeton University Press, Princeton, NJ.
63. Tollrian R, Harvell CD. The Ecology and Evolution of Inducible Defenses. 1999. Princeton University Press, Princeton, NJ.
64. Leao T, Castelão G, Korobeynikov A, Monroe EA, Podell S, Glukhov E, et al. Comparative genomics uncovers the prolific and distinctive metabolic potential of the cyanobacterial genus *Moorea*. *Proc Natl Acad Sci USA* 2017; **114**: 3198–3203.
65. Züst T, Agrawal AA. Trade-Offs Between Plant Growth and Defense Against Insect Herbivory: An Emerging Mechanistic Synthesis. *Annu Rev Plant Biol* 2017; **68**: 513–534.

Figure legends.

Figure 1. Change in (a) cell abundance (cells mL^{-1}), (b) growth rate (d^{-1}), (c) culture nitrate concentration (µM), (d) cell nitrogen content (pg N μm^{-3}), (e) cell carbon content (pg C μm^{-3}), (f) C:N ratio, (g) cell volume (μm^{-3}), (h) cell toxin content (amol μm^{-3}), and (i) the fraction of cells rejected by copepods over time in the batch-culture experiment. Light grey points in (d), (e), (f), and (h) are initial values from the stock culture. Values are means and error bars are standard error (n = 3).

Figure 2. Relation between cellular nitrogen (N, pg N μm^{-3}) or cellular carbon (C, pg C μm^{-3}), and growth rate (GR, d^{-1}) in the (a, b) batch-culture and (c, d) chemostat experiments. Growth rate is calculated from change in biovolume. Multiple linear regression (with 95% confidence intervals) was fit to the data: (a) control: log cell N = −1.594 + 0.420 × GR, induced: log cell N = −1.497 + 0.420 × GR (R^2 = 0.27, p = 0.002); (b) control: log cell C = −0.684 − 0.181 × GR, induced: −0.561 − 0.181 × GR (R^2 = 0.539, $p < 0.001$); (c) control: log cell N = −1.546 + 0.363 × GR, induced: −1.456 + 0.363 × GR (R^2 = 0.28, p <0.001); and (d) control: log cell C = −0.594 – 0.654 × GR, induced: −0.479 – 0.654 × GR (R^2 = 0.61, $p <$ 0.001).

Figure 3. Change in cell abundance (cells mL^{-1}) in the chemostats at the different dilution rates. (a) 0.05 d^{-1}, (b) 0.10 d^{-1}, (c) 0.20 d^{-1} with high (6 nM) and low (0.63 nM) dose of copepodamides, (d) 0.40 d^{-1}. The values are means and error bars show standard error (n = 3). Note the different y-axes scales.

Figure 4. Summary of (a) cell growth rate (d^{-1}), (b) N-specific growth rate (d^{-1}), (c) cell volume ($\times 10^3$ μm^3), (d) cell nitrogen (pg N μm^{-3}), (e) cell carbon (pg C μm^{-3}), (f) C:N ratio, (g) cell toxin content (amol μm^{-3}), and (h) the fraction of cells rejected by copepods in the chemostat experiments. Values are averaged over time during the treatment period and error

559 bars show standard deviation (n = 4 in 0.05, 0.20, 0.40 d^{-1}; n = 5 in 0.10 d^{-1}; n = 3 in 0.10 d^{-1}
560 C/N measurements). Asterisks above bars indicate significant differences between treatments
561 within dilution rates (*** $p < 0.001$, ** $p < 0.01$, * $p < 0.05$). In (j) and all 0.2 d^{-1} high they
562 indicate significant effect of the 'Treatment' factor. Further statistical analysis is reported in
563 the appendix.

564 Figure 5. Relation between copepod rejection rate and cell toxin content (GTX) normalized
565 by volume (amol μm^{-3}). Data are from both batch culture and chemostat experiments. The
566 regression line (with 95% confidence intervals) is Rejection = 0.320 + 0.219 × log GTX (R^2
567 = 0.42, $p < 0.001$). Due to odd behaviour, data from the 0.10 d^{-1} chemostat experiment
568 (triangles) are not included in the regression. Including them does not change the significant
569 effect (R^2 = 12, $p < 0.001$).

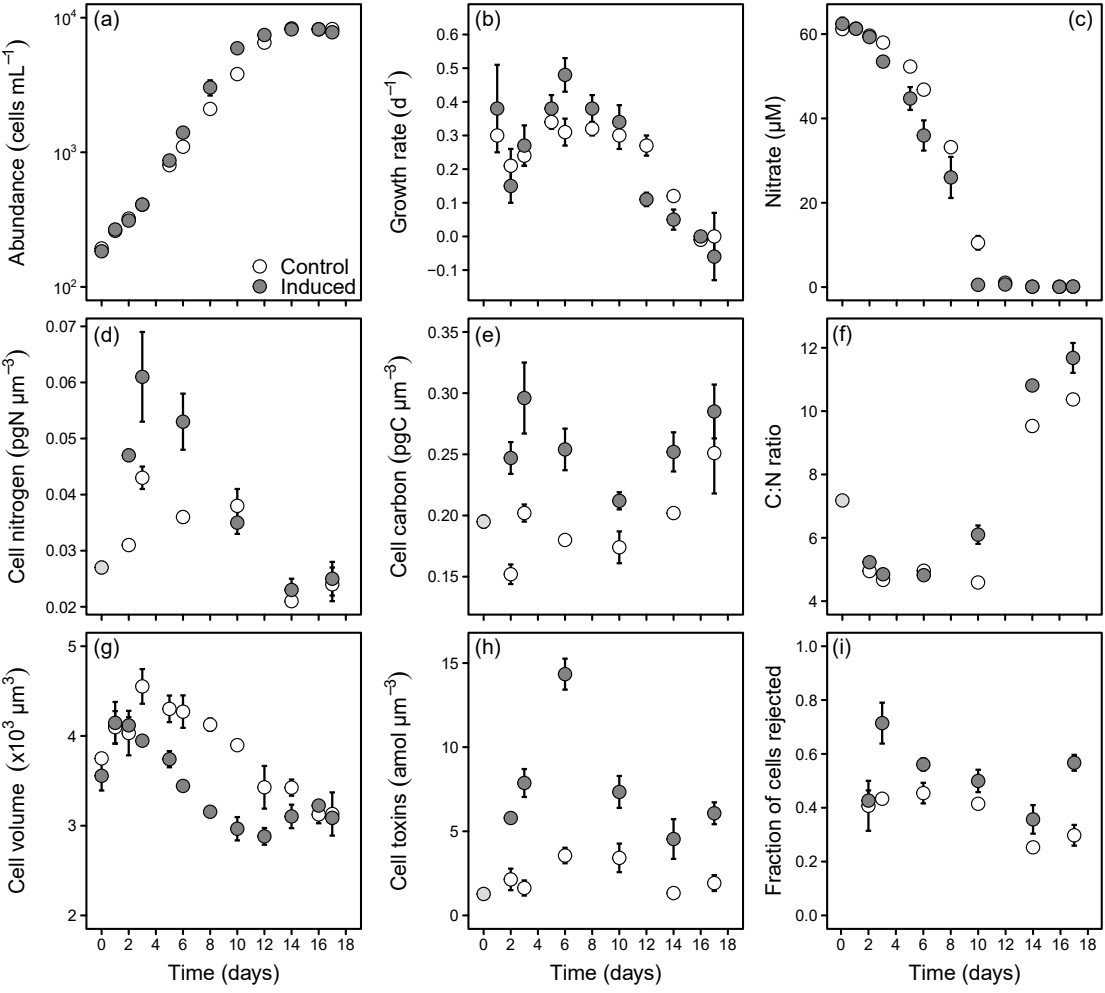
(a)
Abundance (cells mL^{-1})
10^4
10^3
10^2
Control
Induced
(b)
Growth rate (d^{-1})
0.6
0.5
0.4
0.3
0.2
0.1
0.0
−0.1
(c)
Nitrate (µM)
60
40
20
0
(d)
Cell nitrogen (pgN µm^{-3})
0.07
0.06
0.05
0.04
0.03
0.02
(e)
Cell carbon (pgC µm^{-3})
0.35
0.30
0.25
0.20
0.15
(f)
C:N ratio
12
10
8
6
4
(g)
Cell volume (x10^3 µm^3)
5
4
3
2
(h)
Cell toxins (amol µm^{-3})
15
10
5
0
(i)
Fraction of cells rejected
1.0
0.8
0.6
0.4
0.2
0.0
0 2 4 6 8 10 12 14 16 18
Time (days)

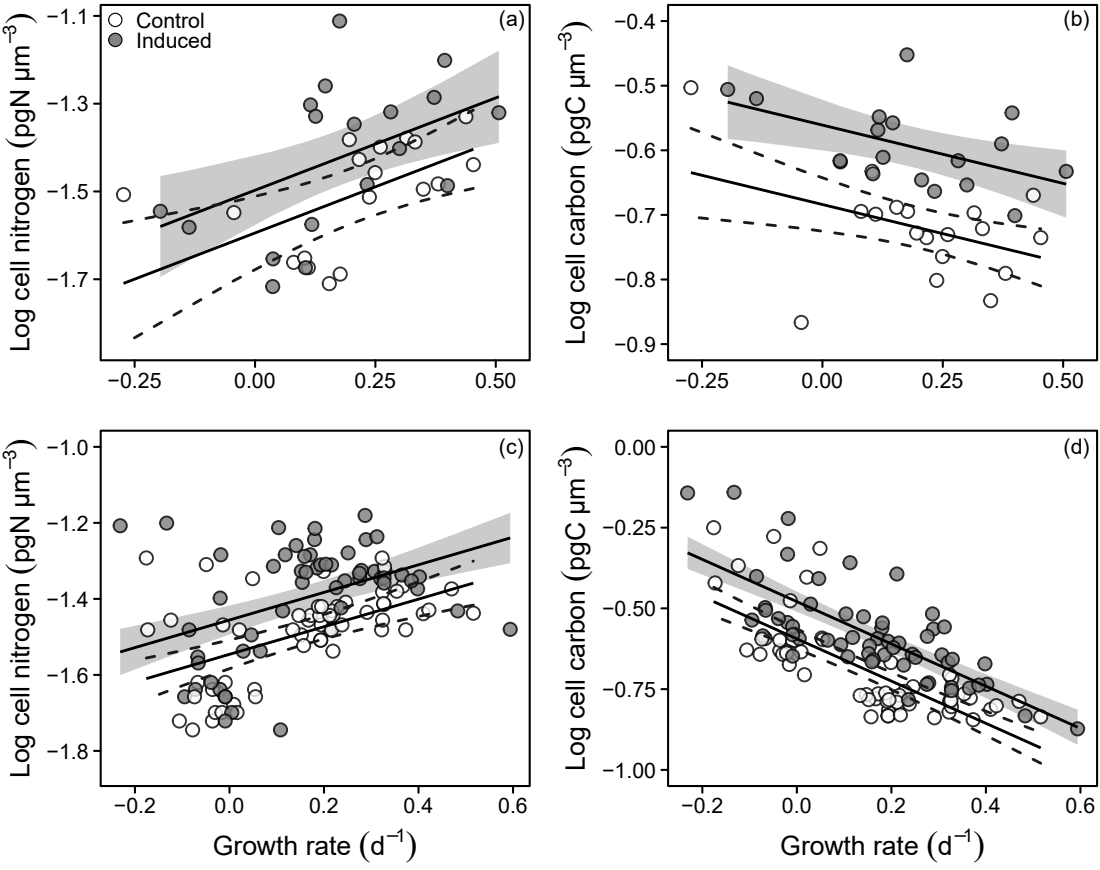
Control
Induced
(a)
(b)
(c)
(d)
Log cell nitrogen (pgN µm^{-3})
Log cell carbon (pgC µm^{-3})
Growth rate (d^{-1})
−1.1
−1.3
−1.5
−1.7
−0.4
−0.5
−0.6
−0.7
−0.8
−0.9
−1.0
−1.2
−1.4
−1.6
−1.8
0.00
−0.25
−0.50
−0.75
−1.00
−0.25
0.00
0.25
0.50
−0.2
0.0
0.2
0.4
0.6

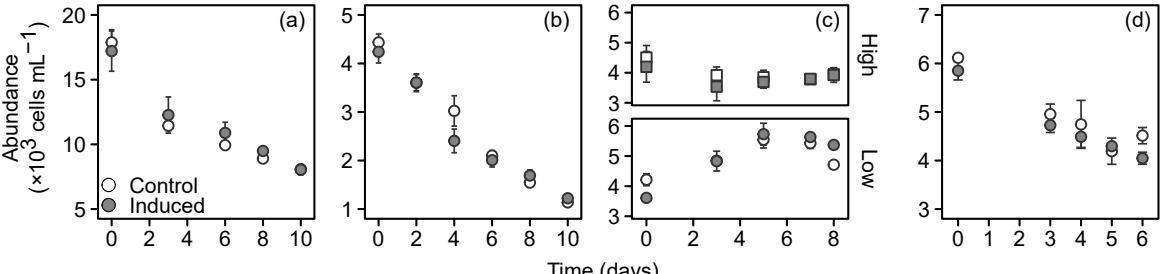
Abundance
(×10^3 cells mL^−1)
(a)
(b)
(c)
(d)
Control
Induced
High
Low
Time (days)

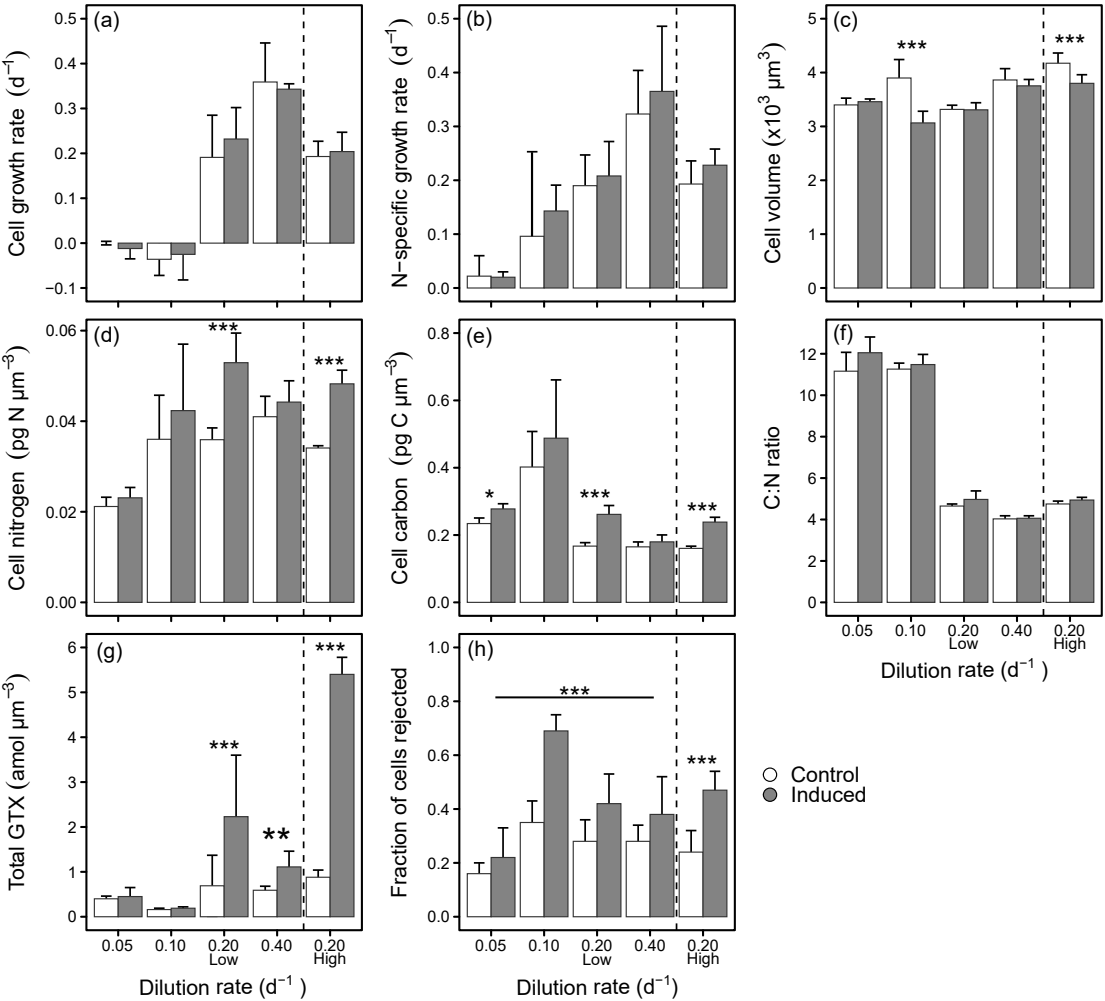
(a)
Cell growth rate (d^{-1})
(b)
N−specific growth rate (d^{-1})
(c)
Cell volume (x10^3 µm^3)
(d)
Cell nitrogen (pg N µm^{-3})
(e)
Cell carbon (pg C µm^{-3})
(f)
C:N ratio
(g)
Total GTX (amol µm^{-3})
(h)
Fraction of cells rejected
0.05
0.10
0.20 Low
0.40
0.20 High
Dilution rate (d^{-1})
Control
Induced

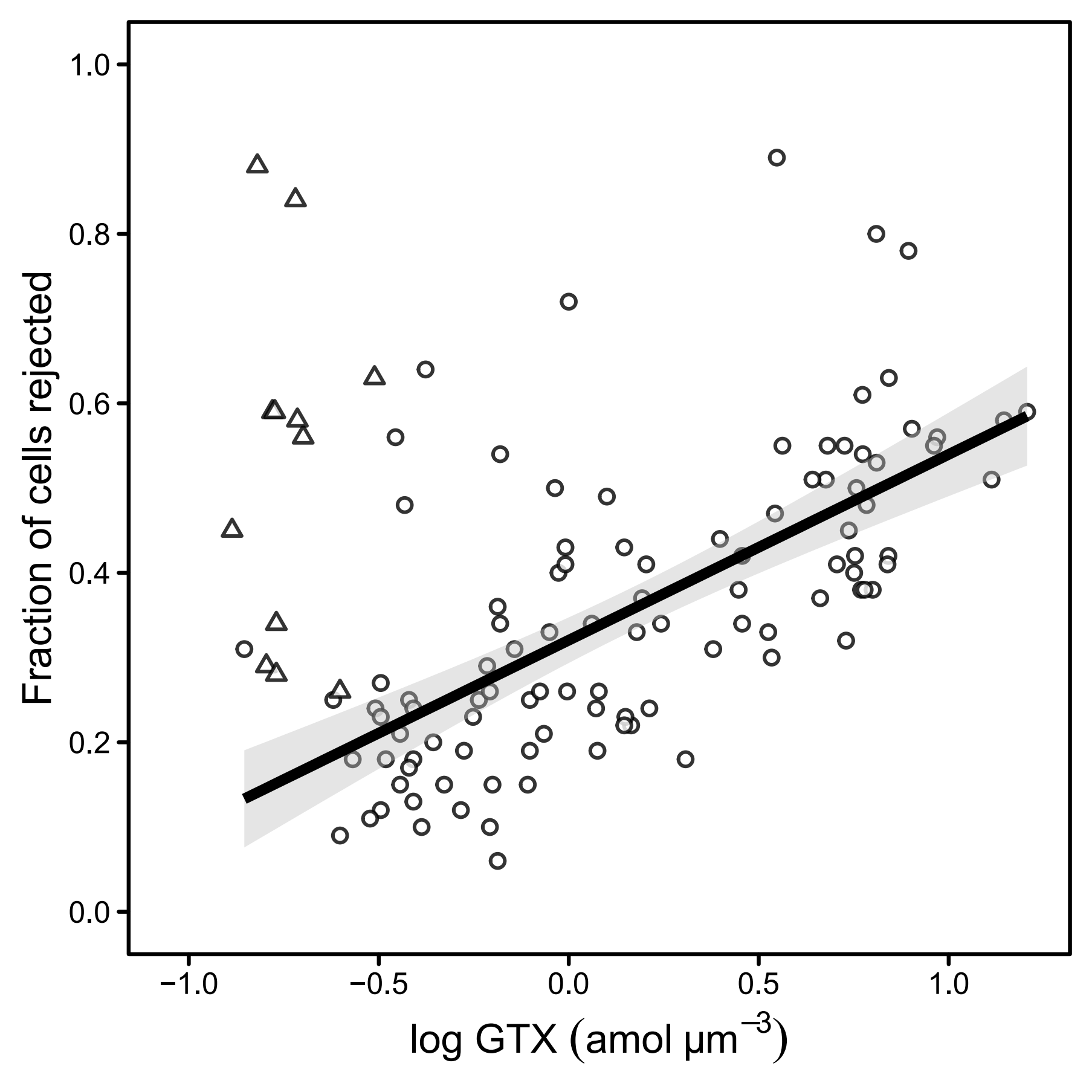
1.0
0.8
0.6
0.4
0.2
0.0
Fraction of cells rejected
−1.0
−0.5
0.0
0.5
1.0
log GTX (amol μm−3)

Supplementary Information

Appendix 1.

The chemostat equation assuming a Michaelis-Menten functional response in nutrient uptake to nutrient concentration reads

$$\frac{dB}{dt} = \mu_{max}\left(\frac{\alpha N(t)}{\mu_{max} + \alpha N(t)}\right)B - DB \tag{1}$$

$$\frac{dN}{dt} = -\mu_{max}\left(\frac{\alpha N(t)}{\mu_{max} + \alpha N(t)}\right)B + D\big(N_i - N(t)\big), \tag{2}$$

where B is the phytoplankton biomass in culture (as cellular mol of nitrogen vol^{-1}), D is the dilution rate (time^{-1}), μ_{max} the maximum growth rate (time^{-1}), α the affinity for nitrate-nitrogen (vol cellular mol of nitrogen^{-1} time^{-1}), N the nutrient concentration in culture (mol N vol^{-1}), and N_i the nutrient concentration in inflow water (mass vol^{-1}). Solving for steady state yields

$$\widehat{N} = \frac{D\mu_{max}}{\alpha(\mu_{max} - D)} \tag{3}$$

$$\widehat{B} = N_i - \frac{D\mu_{max}}{\alpha(\mu_{max} - D)} = N_i - \widehat{N}. \tag{4}$$

While eq. (3) and (4) are two equations with two unknowns (μ_{max}, α), they are not independent and one cannot find both unknowns. With one fixed, one can compute the other.

If the cells respond to a cue by lowering their maximum growth rate and/or its affinity then in the chemostat at steady state the concentration of nutrient will increase, and the density of cells decrease. Assuming first that the response is solely in the maximum growth rate, we can compute the response from the new steady state concentrations, dilution rate, and (known) affinity by solving either eq. (3) or eq. (4) for μ_{max}:

$$\mu_{max} = \frac{\hat{N}\alpha D}{\hat{N}\alpha - D} \text{ or } \mu_{max} = \frac{D\alpha(N_i - \hat{B})}{\alpha(N_i - \hat{B}) - D}. \quad (5)$$

Alternatively, assume that the cells respond by lowering their affinity, then we can similarly compute the response in affinity from the steady state concentrations, the – known or assumed – maximum growth rate, and dilution rate:

$$\alpha = \frac{D\mu_{max}}{\hat{N}(\mu_{max} - D)} \text{ or } \alpha = \frac{-D\mu_{max}}{\hat{B}(\mu_{max} - D) - N_i(\mu_{max} + D)}. \quad (6)$$

Due to the shape of the functional response, these equations do not provide accurate absolute estimates, but do provide estimates of relative changes in maximum growth rate or affinity. However, and unfortunately, for low dilution rates, where according to our hypothesis changes in the parameters in response to grazer cues is expected to be largest, steady state cell concentrations are not very sensitive to changes in the parameters.

Supplementary Information

Appendix 2

Appendix 2 Table S1. Summary statistics for the generalized additive mixed model (GAMM) used to assess the effect of the copepodamide treatment in the batch experiment.

		Estimate	Std. error	t value	*P*
Cell abundance	Intercept	3356.70	124.2	27.02	<0.001
	Treatment	312.10	175.7	1.78	0.081
Growth rate	Intercept	0.22	0.01	15.40	<0.001
	Treatment	−0.01	0.02	−0.27	0.790
Cell volume	Intercept	3844.59	40.24	95.54	<0.001
	Treatment	−397.48	56.91	−6.99	<0.001
Nitrate	Intercept	31.98	0.72	44.22	<0.001
	Treatment	−3.17	1.02	−3.11	0.003
Cell nitrogen	Intercept	0.032	0.001	24.31	<0.001
	Treatment	0.007	0.002	3.97	<0.001
Cell carbon	Intercept	0.193	0.006	30.77	<0.001
	Treatment	0.055	0.009	6.22	<0.001
C:N ratio	Intercept	6.61	0.07	89.99	<0.001
	Treatment	0.63	0.10	6.08	<0.001
Cell toxin	Intercept	2.18	0.33	6.68	<0.001
	Treatment	4.57	0.46	9.88	<0.001
Rejection	Intercept	0.38	0.03	13.82	<0.001
	Treatment	0.15	0.04	3.89	<0.001

Appendix 2 Table S2. Summary statistics for multiple regression analysis on the relationship between log cell nitrogen (pg N μm^{-3}) or log carbon (pg C μm^{-3}), and growth (d^{-1}) in the batch and chemostat experiments. Growth rate is based om change in biovolume (μm^3 mL^{-1}). 'Lower' and 'Upper' refers to 95% confidence intervals.

			Estimate	Std. Error	Lower	Upper	*P*
Batch	Log cell nitrogen	Intercept	−1.594	0.041	−1.677	−1.512	<0.001
		Growth	0.420	0.126	0.164	0.678	0.002
		Treatment	0.097	0.044	0.008	0.187	0.034
	Log cell carbon	Intercept	−0.684	0.020	−0.725	−0.643	<0.001
		Growth	−0.181	0.062	−0.307	−0.054	0.007
		Treatment	0.123	0.022	0.078	0.167	<0.001
Chemostat	Log cell nitrogen	Intercept	−1.546	0.019	−1.584	−1.508	<0.001
		Growth	0.363	0.067	0.230	0.497	<0.001
		Treatment	0.090	0.022	0.045	0.135	<0.001
	Log cell carbon	Intercept	−0.594	0.016	−0.625	−0.563	<0.001
		Growth	−0.654	0.055	−0.764	−0.545	<0.001
		Treatment	0.115	0.017	0.078	0.152	<0.001

Appendix 2 Table S3. Type III analysis of variance (ANOVA) on the fixed effects in the linear mixed models used to analyze the effect of the copepodamide treatment in high dose (6 nM) repeated 0.2 d^{-1} dilution rate chemostat experiment. *P*-values are provided via Satterthwaite's degrees of freedom method. Data on the fraction of rejected cells was log-transformed to homogenize variances.

	Fixed effects	Sum Sq.	NumDF	DenDF	F	*P*
Cell volume*	Treatment	835147	1	21	27.998	<0.001
	Time	431937	1	21	14.480	0.001
Cell growth rate	Treatment	0.0007	1	4	0.21	0.674
	Time	0.0160	1	17	4.84	0.042
N-specific growth rate	Treatment	0.0018	1	4	1.81	0.250
	Time	0.0128	1	17	13.20	0.002
C:N ratio	Treatment	0.0141	1	4	1.005	0.373
	Time	0.1649	1	17	11.691	0.003
Cell toxins	Treatment	41.14	1	4	118.24	<0.001
Log cell nitrogen	Treatment	0.079	1	4	54.66	0.002
Log cell carbon*	Treatment	0.175	1	21	153.22	<0.001
	Time	0.006	1	21	4.83	0.039
Log rejection*	Treatment	0.506	1	19	29.236	<0.001

*: Random effect variances estimated as (close to) zero.

Appendix 2 Table S4. Type III analysis of variance (ANOVA) on the fixed effects in the linear mixed models used to analyze the effect of the copepodamide treatment in low dose (0.63 nM) chemostat experiments. *P*-values are provided via Satterthwaite's degrees of freedom method. Some variables were log-transformed to homogenize variances. DR: dilution rate.

	Fixed effects	Sum Sq.	NumDF	DenDF	F	*P*
Cell volume	Treatment	53547	1	92	0.856	0.356
	Time	380975	1	75	6.117	0.016
	DR	2944857	3	16	15.762	<0.001
	Treatment×Time	35618	1	75	0.572	0.452
	Treatment×DR	2819502	3	16	15.091	<0.001
Cell growth rate*	Treatment	0.0021	1	97	0.334	0.564
	DR	2.6630	3	97	141.219	<0.001
N-specific growth rate*	Treatment	0.0143	1	79	1.580	0.213
	DR	1.5605	3	79	57.564	<0.001
C:N ratio*	Treatment	0.01	1	80	0.016	0.899
	Time	2.91	1	80	8.774	0.004
	DR	912.48	3	80	916.081	<0.001
	Treatment×Time	0.36	1	80	1.093	0.299
	Treatment×DR	2.04	3	80	2.049	0.114
Log cell toxins	Treatment	3.42	1	91	12.29	<0.001
	Time	3.76	1	91	13.50	<0.001
	DR	22.16	3	91	26.55	<0.001
	Treatment×Time	0.85	1	91	3.07	0.083
	Treatment×DR	8.67	3	91	10.38	<0.001
Log cell nitrogen*	Treatment	0.0013	1	80	0.26	0.612
	Time	0.0609	1	80	12.11	<0.001
	DR	1.4240	3	80	94.48	<0.001
	Treatment×Time	0.0053	1	80	1.05	0.309
	Treatment×DR	0.0730	3	80	4.84	0.004
Log cell carbon*	Treatment	0.001	1	80	0.131	0.718
	Time	0.048	1	80	9.755	0.002
	DR	1.006	3	80	68.463	<0.001
	Treatment×Time	0.012	1	80	2.507	0.117
	Treatment×DR	0.858	3	80	5.841	0.001
Log rejection*	Treatment	0.50435	1	57	14.720	<0.001
	DR	1.73364	3	57	16.866	<0.001

*: Random effect variances estimated as (close to) zero.

Appendix 2 Table S5. Summary for chemostat experiments. The values are averaged over time and show means ± standard deviation. DR: dilution rate.

DR	Treatment	Dose	Abundance	Cell growth	N cell mass	N-specific growth	Cell volume	Cell N	Cell C	C:N ratio	Cell toxin	Rejection
d^{-1}			cells mL^{-1}	d^{-1}	µg N mL^{-1}	d^{-1}	$µm^{-3}$	pg N $cell^{-1}$	pg C $cell^{-1}$		fmol $cell^{-1}$	
0.05	Control	Low	9591±1450	0.000±0.004	0.681±0.061	0.022±0.038	3399±126	70.5±5.25	795±40	11.16±0.91	1.28±0.23	0.16±0.04
0.05	Induced	Low	10173±1816	-0.012±0.023	0.806±0.082	0.020±0.010	3459±51	79.8±7.48	956±47	12.05±0.76	1.45±0.69	0.22±0.11
0.10	Control	Low	2282±1022	-0.036±0.036	0.221±0.029	0.096±0.157	3899±343	147±43	1644±448	11.26±0.29	0.63±0.14	0.35±0.08
0.10	Induced	Low	2187±904	-0.025±0.057	0.203±0.108	0.143±0.048	3065±217	131±44	1518±524	11.48±0.49	0.58±0.08	0.69±0.06
0.20	Control	Low	5133±416	0.191±0.094	0.608±0.039	0.190±0.057	3317±78	119±6.9	553±28	4.65±0.10	2.29±2.22	0.28±0.08
0.20	Induced	Low	5391±402	0.232±0.070	0.691±0.087	0.208±0.064	3308±138	160±20	789±79	4.97±0.41	7.16±4.18	0.42±0.11
0.20	Control	High	3942±145	0.193±0.034	0.560±0.014	0.193±0.043	4173±190	142±7.1	669±27	4.75±0.14	3.62±0.76	0.24±0.08
0.20	Induced	High	3738±163	0.204±0.043	0.680±0.036	0.228±0.030	3800±160	183±4.1	903±17	4.94±0.13	21.40±0.90	0.47±0.08
0.40	Control	Low	4611±333	0.359±0.087	0.726±0.090	0.323±0.081	3862±211	158±15	635±49	4.03±0.15	22.7±0.34	0.28±0.06
0.04	Induced	Low	4390±289	0.343±0.012	0.724±0.074	0.365±0.121	3753±119	165±13	670±57	4.06±0.12	4.18±1.31	0.38±0.14

Appendix 2 Table S6. Summary for chemostat experiments, normalized by cell volume to account for differences in size. The values are averaged over time and show ± standard deviation. DR: dilution rate.

DR d^{-1}	Treatment	Dose	Biovolume $\times 10^7\ \mu m^3\ mL^{-1}$	Growth d^{-1}	Cell N pg N μm^{-3}	Cell C pg C μm^{-3}	Cell toxin amol μm^{-3}
0.05	Control	Low	3.269±0.562	-0.011±0.024	0.021±0.002	0.234±0.016	0.40±0.06
0.05	Induced	Low	3.520±0.658	-0.015±0.030	0.023±0.002	0.278±0.015	0.45±0.20
0.10	Control	Low	0.870±0.340	-0.052±0.076	0.036±0.010	0.40±0.11	0.16±0.03
0.10	Induced	Low	0.660±0.256	-0.066±0.120	0.042±0.015	0.48±0.17	0.19±0.03
0.20	Control	Low	1.705±0.113	0.217±0.042	0.040±0.003	0.167±0.01	0.69±0.68
0.20	Induced	Low	1.783±0.166	0.234±0.038	0.053±0.007	0.261±0.03	2.23±1.37
0.20	Control	High	1.644±0.048	0.208±0.024	0.034±0.001	0.160±0.01	0.88±0.16
0.20	Induced	High	1.421±0.111	0.203±0.064	0.048±0.003	0.238±0.01	5.40±0.38
0.40	Control	Low	1.772±0.066	0.372±0.043	0.041±0.005	0.165±0.01	0.59±0.09
0.40	Induced	Low	1.651±0.141	0.340±0.053	0.044±0.004	0.180±0.02	1.11±0.35

Appendix 2 Figure S1.

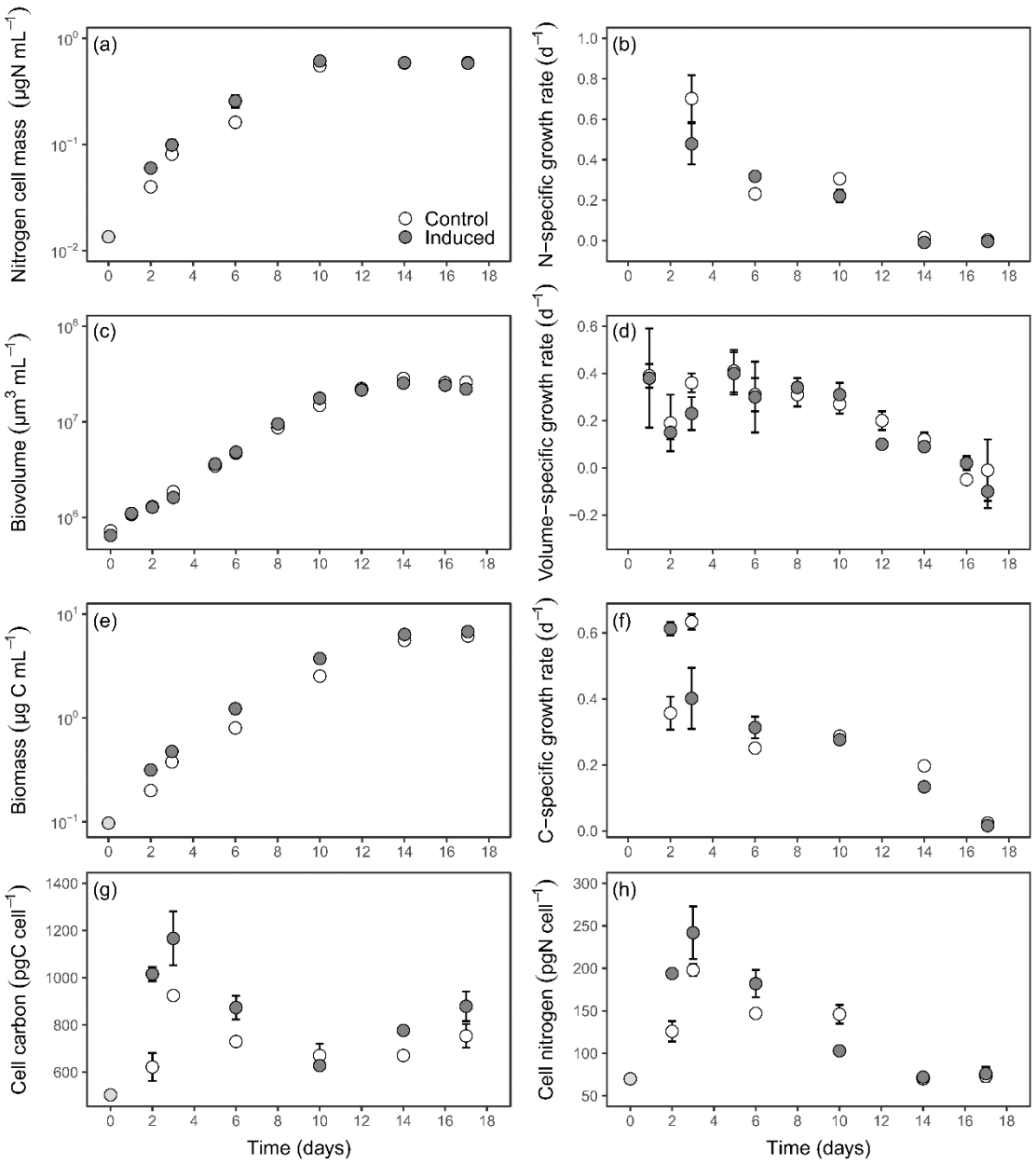

Figure S1. Change in (a) cell-bound nitrogen (µg N mL^{-1}), (b) N-specific growth rate (d^{-1}), (c) biovolume (μm^3 mL^{-1}), (d) volume-specific growth rate (d^{-1}), (e) biomass (µg C mL^{-1}), (f) C-specific growth (d^{-1}), (g) cellular carbon (pg C $cell^{-1}$), and (h) cellular nitrogen (pg N $cell^{-1}$), over time in the batch culture experiment. The grey points in (a), (e), (g) and (h) are initial values taken from the stock culture. Values are means and error bars show standard error (n = 3).

Appendix 2 Figure S2.

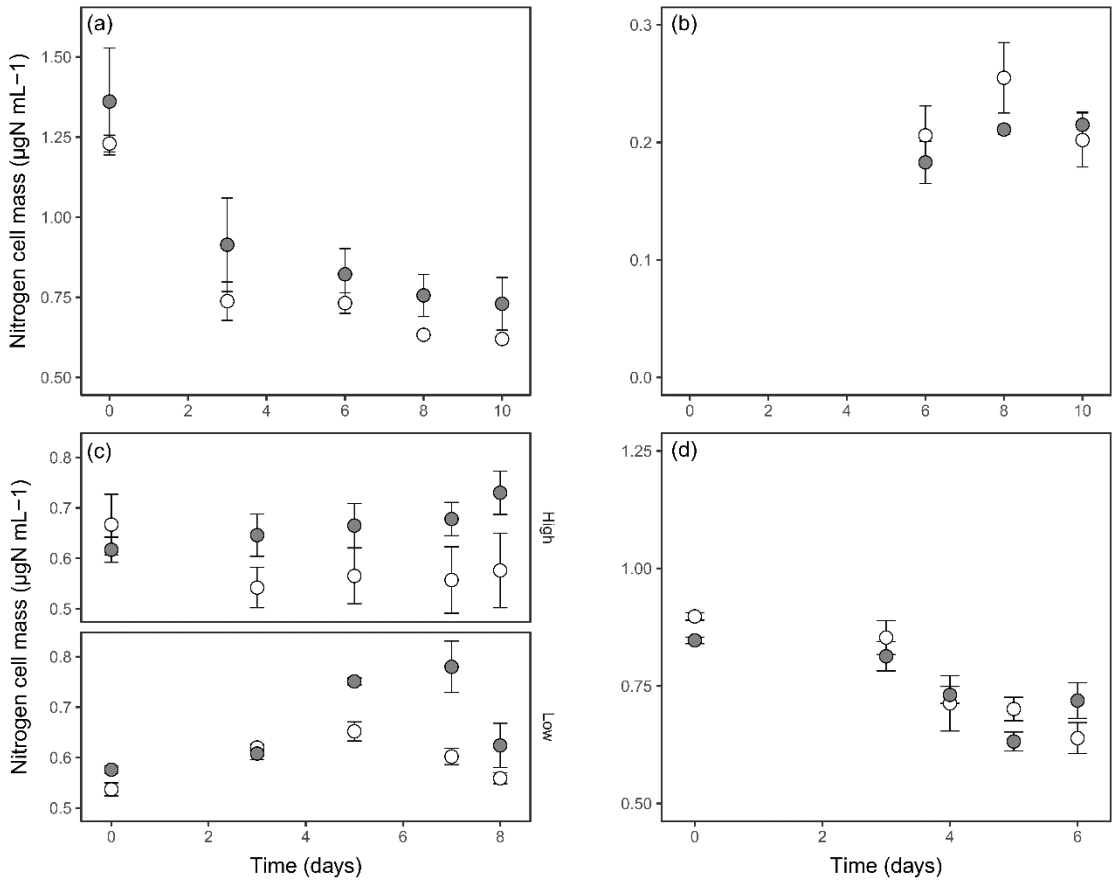

Figure S2. Change in cell-bound nitrogen (µg N mL^{-1}) in the chemostat at the different dilution rates. (a) 0.05 d^{-1}, (b) 0.10 d^{-1}, (c) 0.20 d^{-1} with high (6 nM) and low (0.63 nM) dose of copepodamides, (d) 0.40 d^{-1}. The values are means and error bars show standard error (n=3). Note the different y-axes scales.

Appendix 2 Figure S3.

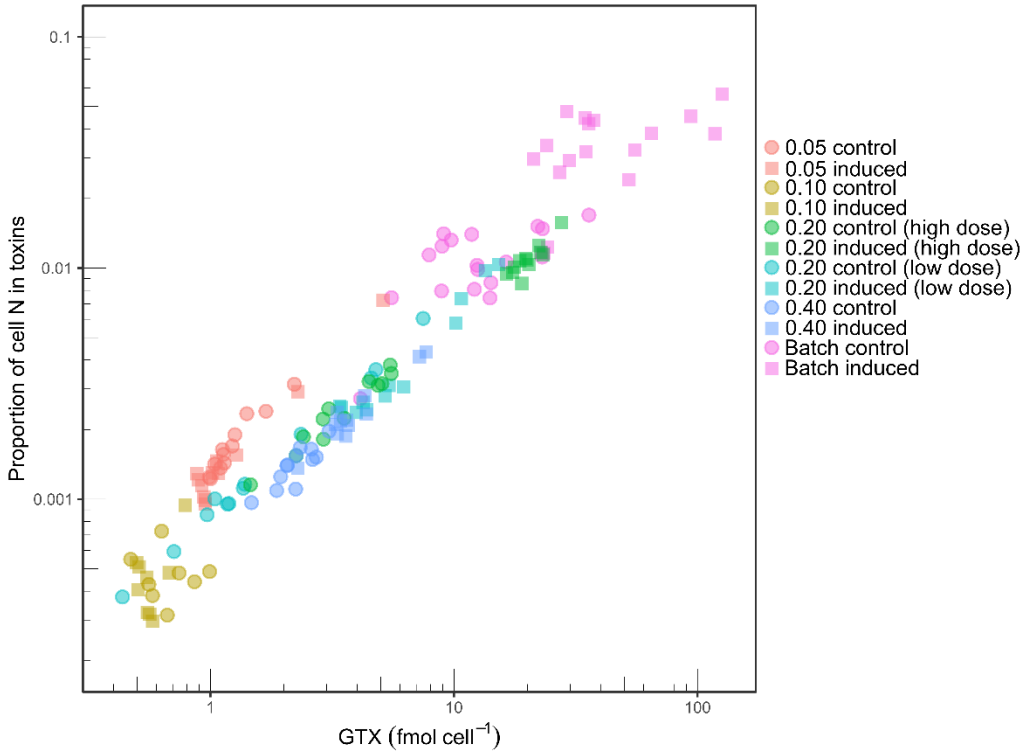

Figure S3. Relation between the proportion of cell nitrogen invested in toxins as a function of the cell toxin content (fmol cell^{-1}).

Supplementary Information

Appendix 3. Dose-response experiment

We performed a dose-response experiment to determine toxin-induction potential of different copepodamide concentrations. Triplicate *Alexandrium minutum* cultures were exposed to four different nominal concentrations (0, 1, 5, 10 nM) of copepodamides under the same conditions as the stock cultures. After 48 hours cells were extracted for toxin analysis as described in the methods section. Cell concentrations were determined using a Beckman Coulter Multisizer 3 (Brea, California, USA).

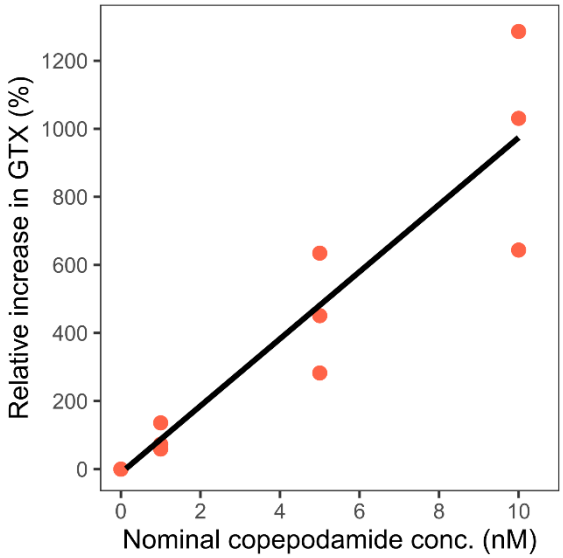

Figure S1. Relation between nominal copepodamide (Ca) concentration (nM) and the increase in cell toxin content relative to the controls in the dose-response experiment. The regression line is $-11.02 + 98.52 \times Ca$ ($R^2 = 0.854$, $p < 0.001$).